

Study on the standard of the four relationships of reservoir and the lower limit of effective reservoir in Nantun Formation of Oilfield A

Yalou Zhou ¹, Guangjuan Fan ^{1,2}, Ang Gao ¹, Wentong Zhao ¹, Ting Dong ¹

¹ School of Earth Science, Northeast Petroleum University, Daqing 163318, China;

² Key Laboratory of Reservoir Formation Mechanism and Resource Evaluation of Heilongjiang Province, Daqing 163318, China

Abstract. By using the data of logging, cuttings logging, thin section identification and analysis in the study area to study the four characteristics of the Nantun Formation reservoir and their relationship, the lower limit standard of effective reservoir physical property is established by the logging interpretation model of the reservoir mud content, porosity, permeability and saturation, and the mercury injection method, oil production method, oil test analysis method and cumulative frequency statistics method. The lower limit standard of effective reservoir electrical property is determined by using fluid identification chart. The results show that the lithology of the second member of Nantun Formation is mainly sandy conglomerate, and the first member of Nantun Formation is mainly sandstone, and the sandstone is more developed. The oil content is mainly full of oil, oil spots and oil stains. The reservoir porosity is between 4~20% and permeability is 0.01~100 mD, showing low porosity and low permeability. The lower limit of effective reservoir in Nantun Formation is porosity of 7%, permeability of 0.05mD, sonic time difference of 63 μ s/ft, density of 2.55 g/cm³ and water saturation of 20%.

Keywords: Wuerxun Sag; Nantun Formation; Four-property relationship of the reservoir; log interpretation model; standard for lower limits of effective reservoir.

1. Introduction

An oilfield is located in the Wuerxun depression in the central fault depression zone of the Hailaer Tamchage basin in China. The strata of the Tamulanhe Formation, Tongbomiaoh Formation, Nantun Formation, Damoguaihe Formation, Yimin Formation, and Qingyuangang Formation developed in the Lower Cretaceous. Three sets of reservoir cap assemblages are developed, with the Nantun Formation in the middle assemblage being the most abundant in oil and gas. The Damoguaihe Formation is a regional cap rock, while the Nantun Formation is the main source rock and reservoir. Mudstones in the study area are mostly grayish green, dark gray, and black in color, representing the underwater sedimentary environment. With little or no gravel, and high compositional and structural maturity, it represents a medium to low energy underwater sedimentary environment. Wedge shaped cross bedding, trough shaped cross bedding, deformed bedding, and ball pillow structures are developed, and unknown scouring surfaces are common. The sand body is relatively well sorted, with a fine particle size, and has traction current deposition characteristics with a certain transportation distance. The C-M diagram shows that progressive suspension

transportation is the main body, followed by uniform suspension transportation and rolling transportation. Particles are characterized by uniform suspension and progressive suspension, and reservoir sedimentation is dominated by traction flow transportation mechanism. The provenance direction of the target layer mainly comes from the north of the research area, which is in the northeast or northwest direction within the development area. The target layer is braided river delta front subfacies deposition, mainly developing sedimentary microfacies such as underwater channel, mat bar, mat sand, and interdistribution, with sand bodies mainly concentrated in underwater channel microfacies. The relationship between the four characteristics of a reservoir (lithology, electrical property, physical property, and oil bearing property) and the determination of the effective reservoir lower limit are of practical significance for oil and gas exploration and development. Previous studies on the sedimentary characteristics of the study area have yielded sufficient results, but there has been no systematic study on the four characteristics of the reservoir in the study area and how to determine the lower limit criteria for effective reservoirs. This paper uses data from logging, cuttings logging, thin section identification, and analytical testing in the study area to study the four relationships of the

Nantun Formation, and establishes a reservoir logging interpretation model to determine the effective reservoir lower limit standard.

2. Study on the four characteristics and relationship of reservoir

2.1 Four characteristics of reservoir

(1) Lithological characteristics of the reservoir. Based on the analysis of core and logging data from 8 core wells in the study area, it is shown that the main lithology of the reservoir in the South Second Member is sandy conglomerate, while the main lithology of the reservoir in the South First Member is siltstone and fine sandstone. Compared to the two, sandstone is more developed. The particles of lithic sandstone are mainly sub angular to sub circular and of particle supported type. The proportion of rock debris in the rock particles is 29.2%, the proportion of quartz is 24.7%, the proportion of feldspar is 23.8%, and the proportion of filler is 22.3%. Among them, the muddy filling material is 18%, and the carbonate filling material is 4.3%.

(2) Oil bearing characteristics of the reservoir. Based on the analysis of oil bearing core sections and cuttings logging data from 8 core wells in the study area, it is shown that the oil bearing grades of the Nantun Formation are mainly divided into five categories: saturated oil, oil immersion, oil spots, oil traces, and fluorescence, with saturated oil accounting for 21% and oil immersion accounting for 10%; Oil spots accounted for 26%; Oil stains accounted for 22%, and fluorescence accounted for 21%. The main oil bearing grades of the Nantun Formation are saturated oil, oil spots, and oil traces.

(3) Reservoir physical characteristics. According to the histogram of the shale content of the reservoir in the Nantun Formation, the shale content of the reservoir in the South 2nd Member (Figure 1) mainly ranges from 10% to 30%; The main range of the South First Member (Figure 2) is between 10% and 20%. Compared to the two, the mud content of the South Second Member reservoir is higher. According to the distribution histogram of porosity and permeability of the Nantun Formation (Figure 3-6), it can be seen that the porosity of the reservoir in the Nantun Formation is mainly concentrated in 4% ~ 20%, and the permeability is mainly in 0.01mD~100mD; The porosity and permeability of the South 1st Member is better than that of the South 2nd Member, and the Nantun Formation is a low porosity and low permeability reservoir.

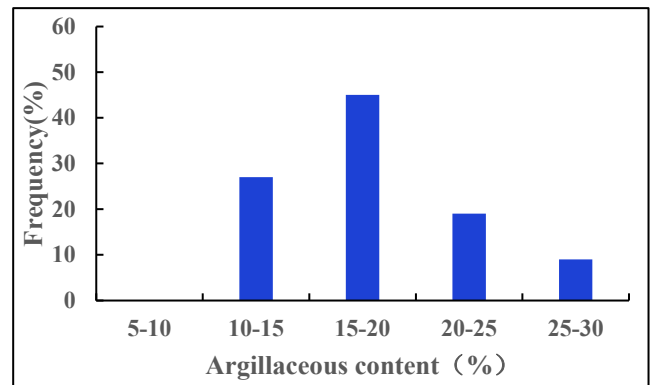


Fig.1 Distribution histogram of mud content in South Section II

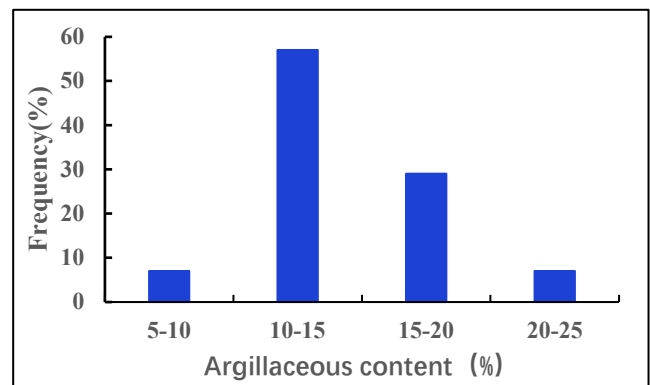


Fig.2 Distribution histogram of mud content in South Section I

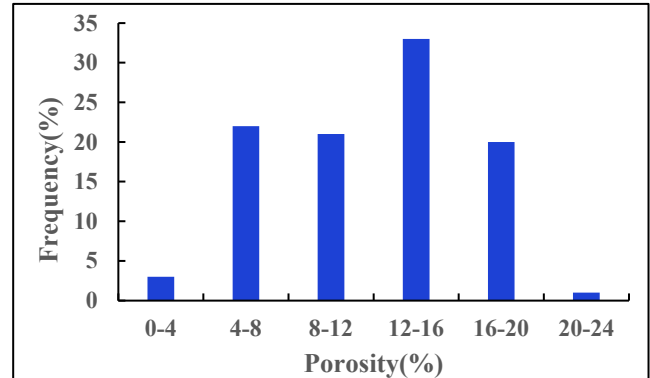


Fig.3 Porosity Distribution Histogram of South Section II

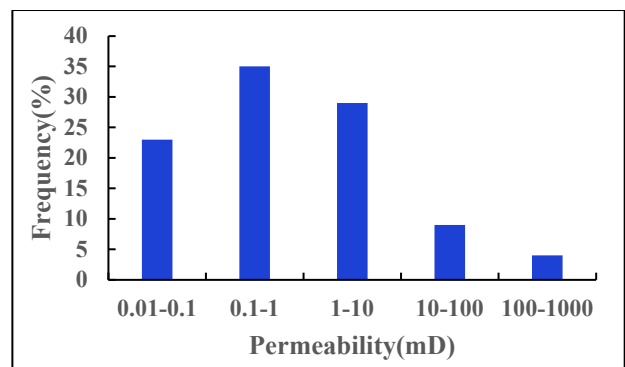


Fig.4 Permeability Distribution Histogram of South Section II

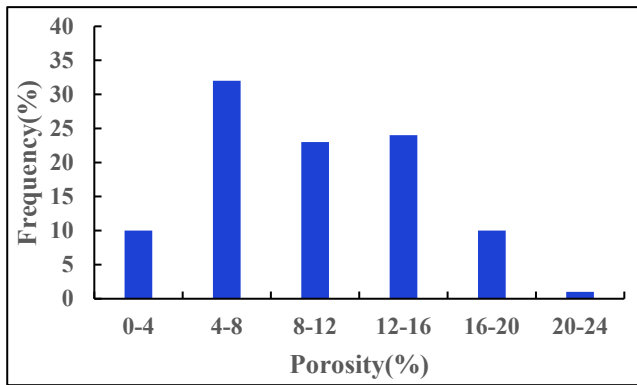


Fig.5 Porosity Distribution Histogram of South Section I

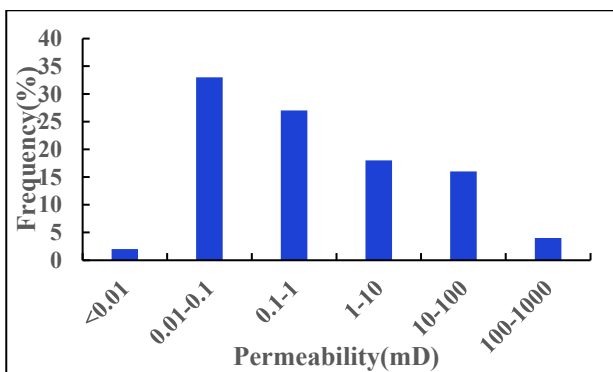


Fig.6 Permeability Distribution Histogram of South Section I

(4) Reservoir electrical characteristics. Reservoir lithology, oil bearing property, and physical property characteristics all have an impact on reservoir electrical properties. Based on the analysis of core well X27, it is found that both layer 113 and layer 115I of well X27 are oil layers. The resistivity amplitude value is large and the oil content is good; Low density, high neutron value, high porosity.

Layer 113: The natural gamma ray is 119.6 API, the shallow lateral resistivity is 32 $\Omega \cdot m$, the compensated neutron is 17.1%, the compensated density is 2.39 g/cm^3 , and the acoustic transit time is 74.8 $\mu s/ft$.

Layer 115: The natural gamma ray is 119.6 API, the shallow lateral resistivity is 32 $\Omega \cdot m$, the compensated neutron is 17.1%, the compensated density is 2.39 g/cm^3 , and the acoustic transit time is 74.8 $\mu s/ft$.

2.2 Relationship between four reservoir properties

(1) The relationship between lithology and oil bearing property. According to the distribution histogram of lithology and fluid types (Figure 7), it can be seen that the oil content of reservoirs is mainly concentrated in sandstone and glutenite reservoirs, with about 79% of the sandstone reservoirs containing oil, and only about 21% of the sandstone reservoirs containing water or dry layers. From the oil level and lithology distribution diagram (Figure 8), it can be seen that the main oil content levels of glutenite are oil immersion and a small amount of oil stains, and the oil content levels of sandstone are saturated oil, oil stains, and oil stains Oil bearing and fluorescence,

from which it can be seen that the oil bearing grade of sandstone is higher than that of conglomerate.

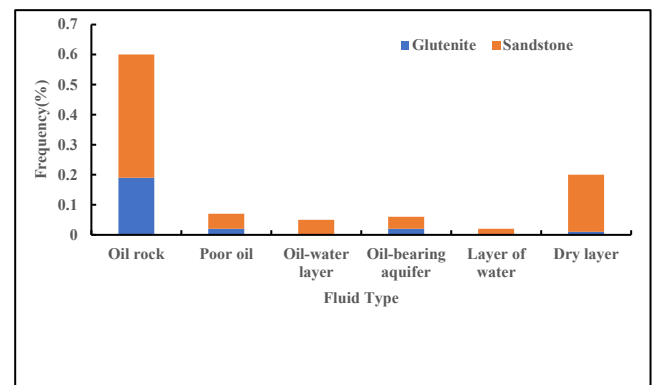


Fig.7 Relationship between lithology and fluid type

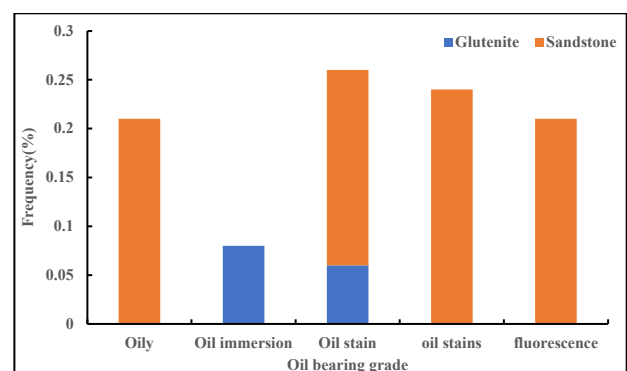


Fig.8 Relationship between lithology and oil grade

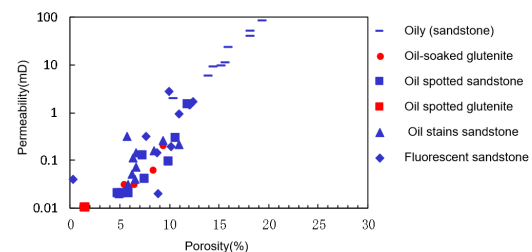


Fig.9 Cross plot of porosity and permeability of different oil-bearing occurrences

(2) The relationship between physical properties, lithology, and oil bearing properties. From the intersection diagram of porosity and permeability for different oil bearing occurrences (Figure 9), it can be seen that the better the physical properties of the reservoir (the higher the porosity and permeability value), the better the lithology and oil content of the reservoir. The physical properties of sandstone are better than those of sandy conglomerate, and lithology controls the physical properties; For sandstone, the porosity and permeability values of oil rich and oil stain are relatively high, while for oil stain and fluorescence, the overall porosity and permeability values are relatively low.

3. Logging interpretation model for reservoir parameters

3.1 Interpretation model of shale content

According to the research on the relationship between the four properties, the shale content of the reservoir is between 10% and 25% in both the South 1st and South 2nd Member. Overall, the shale content is relatively heavy, so it is necessary to consider the impact of the shale content on the calculation of reservoir parameters. Using natural gamma curve to calculate the shale content is not affected by fluid properties, which is the most common method. The specific formula is as follows (Equation 1~2):

$$V'_{sh} = \frac{GR - GR_{min}}{GR_{max} - GR_{min}} \quad (1)$$

$$V_{sh} = \frac{2^{Gcur} \cdot V'_{sh} - 1}{2^{Gcur} - 1} \quad (2)$$

V_{sh} —Shale content, %; GR —Natural gamma, API; GR_{max} —Natural gamma value at mudstone, API; GR_{min} —Natural gamma value at sandstone, API; $Gcur$ —Stratigraphic age coefficient, 2.0 for old formation.

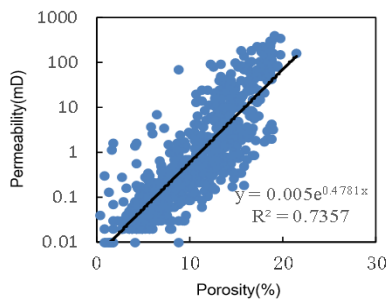


Fig.10 Porosity interpretation model

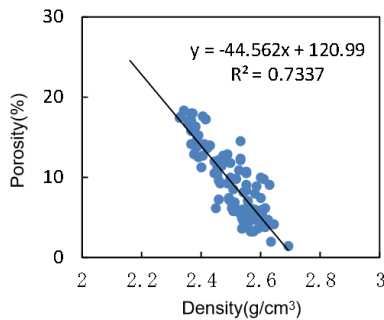


Fig.11 Permeability interpretation model

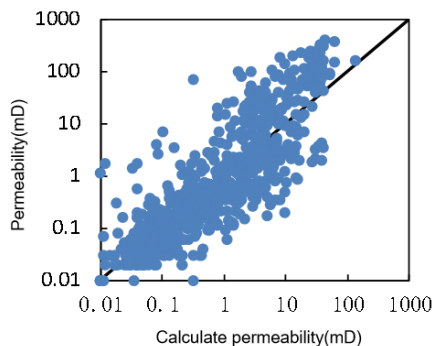


Fig.12 Accuracy analysis of permeability model

3.2 Porosity interpretation model

The reservoir lithology of South 1 and South 2 is mainly composed of sandstone and glutenite, while the core data is mainly from South 1. Therefore, a unified porosity model should be established to calculate the porosity of sandstone and glutenite reservoirs. Firstly, the core is deeply positioned. On this basis, a quantitative interpretation model for porosity in the study area is established using core analysis porosity and acoustic, neutron, and density regression methods, and the density method is preferred for porosity calculation. The regression formula is shown in Formula 3. From Figure 10, it can be seen that there is a good relationship between density and porosity, with a correlation coefficient of 0.86.

$$Y = 44.562x + 120.99; R^2 = 0.7337 \quad (3)$$

3.3 Permeability interpretation model

Permeability is an important parameter reflecting the permeability of a reservoir, which is closely related to the pore structure of rocks. For rocks with little change in pore structure, there is a good correlation between permeability and porosity, and this relationship can be used to estimate reservoir permeability through porosity. Using the method of core analysis porosity and permeability regression to establish a permeability interpretation model (Figure 11), the regression equation is shown in Formula 4; Figure 12 shows the intersection diagram of model calculated permeability and core analysis permeability. From the intersection diagram, it can be seen that the distribution of permeability is on the 45 degree line, indicating that the model can be used for the quantitative interpretation model of permeability in the Wuerxun area.

$$Y = 0.005e^{0.4781x}; R^2 = 0.7337 \quad (4)$$

3.4 Saturation interpretation model

Aiming at the characteristics of low porosity and low permeability in the reservoir of the Nantun Formation, this paper selects the Archie formula to establish a reservoir saturation model. For the Archie formula, the first thing to determine is the value of the formation water resistivity.

(1) Determination of formation water resistivity

According to the analysis data of water samples from the Nantun Formation (Table 1), it can be seen that the equivalent sodium chloride mineralization of the South Second Member is mainly distributed between 12385~20172 ppm, with an average value of 16315 ppm; For the southern section, the equivalent sodium chloride mineralization is mainly distributed in 11218~23315 ppm, with an average value of 20203 ppm. Using the formation water salinity combined with Formula 5, it is determined that the formation water resistivity of the South Second Member is 0.12 $\Omega \cdot m$, and the formation water resistivity of the South First Member is 0.08 $\Omega \cdot m$.

Tab.1 Data Table of Mineralization Distribution of Formation Water in the Study Area

| Layer | Range of mineralization | Equivalent Nacl mineralization range | Average value of equivalent nacl mineralization |
|-----------------|-------------------------|--------------------------------------|---|
| South Section 2 | 22636.95~40099.27 ppm | 12385.23~20171.67 ppm | 16314.19 ppm |
| South section 1 | 11218.32~23123.80 ppm | 11218.32~23314.58 ppm | 20203.1 ppm |

$$R_w = 82 * (10^{3.562 - 0.955 * \lg P_w + 0.0123}) / (1.8 * T + 39) \quad (5)$$

R_w—Formation water resistivity, Ω·m; P_w—Mineralization degree, ppm; T—Temperature, °C.

(2) Determination of saturation parameters

Using the electrical experimental data of sandstone and glutenite in the study area, study the relationship diagram between formation factors, porosity, and resistivity increase coefficient, water saturation (Figure 13~14). Under dual logarithmic coordinates, they are linear characteristics. Therefore, use the regression formula as the value of the saturation parameter in the study area, namely, a=1.233, b=0.85, m=1.556, n=1.967.

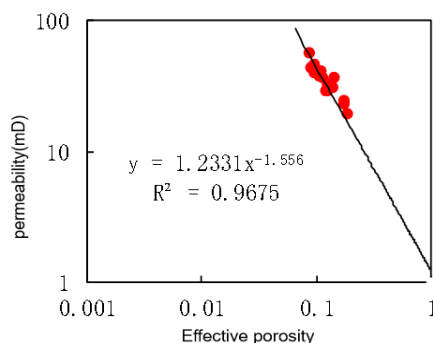


Fig.13 Cross plot of formation factors and porosity

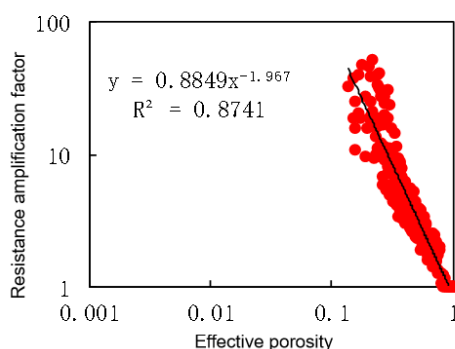


Fig.14 Cross plot of resistance increase coefficient and water saturation

(3) Resistivity forward modeling

The rock electrical parameter values established using rock electrical experimental data, combined with the formation water resistivity values, are substituted into the Archie formula to obtain a chart for resistivity forward simulation. The collected oil testing data are placed on the resistivity simulation line, and the saturation limits for each fluid type are determined. For oil reservoirs, the water saturation is less than 50%; The water saturation of the same oil water layer is greater than 50% and less than 70%; The water saturation of the oil bearing water layer is greater than 70% and less than 80%; The water saturation of the water layer is greater than 80%.

4. Determination of the lower limit of effective reservoir

The determination of the lower limit of effective oil and gas reservoirs is a key task for oil and water reservoir identification, reserve calculation, and development plan formulation. This study mainly uses data such as core testing and analysis, logging, and oil testing and production testing to determine the lower limit value of effective reservoirs through statistical analysis, construction of relationship diagrams, and other means. It mainly uses mercury intrusion method, oil occurrence method, oil testing analysis method, cumulative frequency statistics, and fluid identification charts to establish the lower limit standard of effective reservoirs.

4.1 Determination of reservoir lower limit by mercury intrusion method

Generally, capillary pressure curves and test data obtained from mercury intrusion experiments are used to analyze the microscopic pore structure characteristics of rocks to obtain the minimum flow pore throat radius. Based on the minimum flow pore throat radius, the corresponding porosity and permeability values, namely the lower limit value of reservoir physical properties, are further calculated.

The size of the minimum flow pore radius is mainly determined by the cumulative contribution rate of permeability. It is generally believed that the corresponding pore throat radius when the cumulative contribution rate of permeability reaches 99% is the minimum flow pore throat radius. Therefore, through statistical mercury intrusion data in the study area, the corresponding pore throat radius when the cumulative contribution rate of permeability of each rock core is 99% is obtained. Through statistics, it is determined that the minimum flow pore radius is 0.016 μm (Figure 15). By establishing the intersection diagram of pore radius and porosity for each rock sample (Figure 16) and the intersection diagram of pore radius and permeability (Figure 17), it is determined that the lower limit determined using mercury intrusion data is porosity equal to 7.4% and permeability equal to 0.05mD.

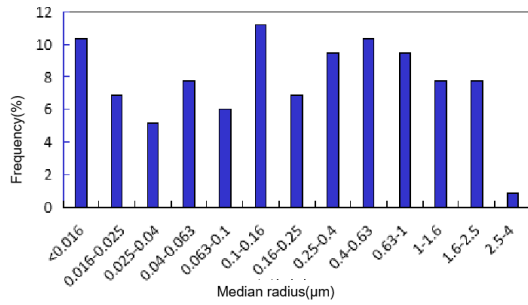


Fig.15 Median radius distribution map

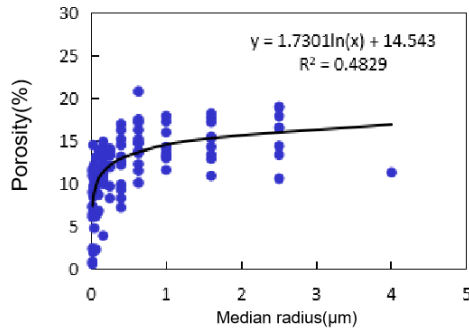


Fig.16 Cross plot of median radius and porosity

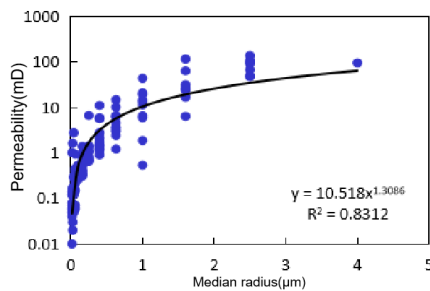


Fig.17 Cross plot of median radius and permeability

The oil testing method is to use the data of oil testing and core physical property analysis to determine the lower limit of physical property by constructing a cross plot of porosity and permeability for dry layers (non effective reservoirs) and producing layers (effective reservoirs), and using the porosity and permeability values corresponding to the boundary between the dry layers and producing layers. Due to the small amount of core data available at the oil testing horizon, the porosity of the reservoir is inversely calculated using the reservoir and dry layer logging response limits of sandstone and glutenite, and the permeability of the oil testing horizon is determined using a permeability model. The corresponding lower limit for the reservoir is that the porosity is equal to 5.7%, and the permeability is equal to 0.08mD.

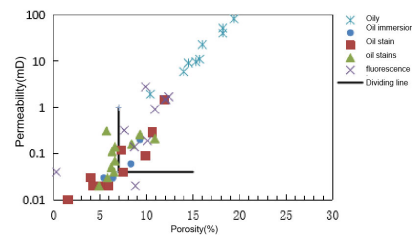


Fig.18 Cross plot of permeability and porosity by oil occurrence method

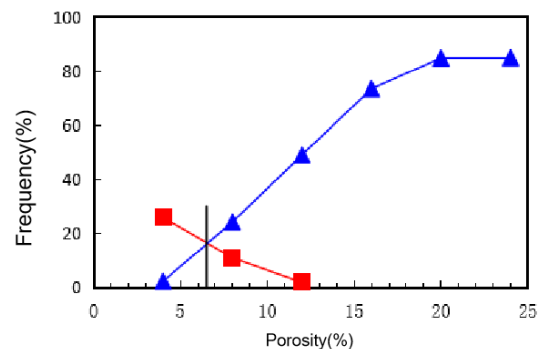


Fig.19 Schematic Diagram for Determining Lower Limit of Reservoir by Cumulative Frequency Method

4.2 Determination of reservoir lower limit by oil bearing occurrence method

Based on the different levels of oil occurrence descriptions of logging cores and cuttings corresponding to different oil production capabilities, reservoirs described as saturated with oil, rich in oil, immersed in oil, or spotted with oil are classified as industrial oil layers, reservoirs with oil spots or traces are classified as low producing oil layers, and reservoirs with fluorescence and no display are classified as dry layers. The oil bearing occurrence method selected in this article mainly uses the porosity and permeability data from the physical property analysis of the core of the target layer to construct the porosity and permeability intersection diagram for different oil bearing grades (Figure 18), and determines the lower limit value of the reservoir physical property based on the boundary between the industrial oil layer and the low production oil layer. The limits determined using this method are porosity equal to 7.0% and permeability equal to 0.04mD.

4.3 Determination of reservoir lower limit by oil testing analysis

4.4 Determination of reservoir lower limit using cumulative frequency statistics

This method utilizes the permeability limit determined above of 0.04mD, forward accumulation of coring data greater than 0.04mD, and reverse accumulation of coring data less than 0.04mD. The intersection of the forward and reverse accumulation curves is used as the boundary for determining whether the reservoir physical properties are effective. Figure 19 shows the sample distribution frequency greater than 0.04mD and the sample distribution frequency less than 0.04mD, with the intersection point of 6.5%. Therefore, the lower limit determined by this method is that the porosity is equal to 6.5% and the permeability is equal to 0.04mD.

4.5 Determining the lower limit of reservoir electrical property using fluid identification chart

The qualitative identification of fluid types mainly starts with oil testing data, and determines the differences in electrical characteristics of oil and water layers based on the study of the four characteristics. By summarizing the logging responses sensitive to fluids, the qualitative identification of fluid types is achieved using cross plot technology.

Based on real-time while drilling curves, compensated neutron, compensated density, acoustic transit time, and other logging curves that are sensitive to oil and water layers, a qualitative identification chart for oil and water layers has been established (Figure 20~21), thereby determining that the lower limit standard for acoustic transit time is 63 $\mu\text{s}/\text{ft}$, the lower limit standard for density is 2.55 g/cm^3 .

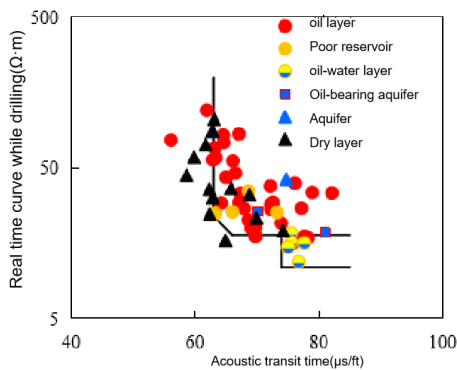


Fig.20 RT-AC Fluid Identification Plate

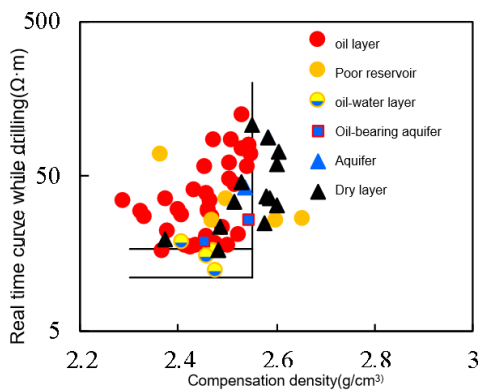


Fig.21 RT-DEN Fluid Identification Plate

Comprehensive mercury injection method, oil bearing occurrence method, oil testing analysis method, and cumulative frequency statistics method have established the lower limit standard for reservoir physical properties. Combined with the fluid identification chart, the lower limit standard for reservoir electrical properties has been determined, and the lower limit discrimination standard for the reservoir in the study area has been established (Table 2).

Tab.2 Standard Data Sheet for Lower Limit of Effective Reservoir

| Reservoir logging response | Porosity/% | Permeability/mD | Acoustic transit time/ ($\mu\text{s}/\text{ft}$) | Density/(g/cm^3) | Water saturation/% |
|----------------------------|------------|-----------------|---|------------------------------------|--------------------|
| Lower limit standard | 7 | 0.05 | 63 | 2.55 | 20 |

5. Conclusion

(1) By using core logging data, cuttings logging data, thin section identification data, and analytical testing data in the study area to analyze the characteristics and relationships of the four reservoir properties (lithology, physical property, electrical property, and oil bearing property) of the Nantun Formation, the study indicates that the lithology of the second member of the Nantun Formation is mainly sandy conglomerate. The southern section is mainly composed of sandstone; The main oil-bearing properties are saturated oil, oil spots, and oil stains; The porosity of the reservoir is about 4~20%, and the permeability is about 0.01~100mD. The reservoir is a low porosity and low permeability reservoir; The electrical properties of oil bearing reservoirs are characterized by large resistivity amplitude values and good oil bearing properties; Low density, high neutron value, and high porosity. The lithology and physical properties of the reservoir are positively correlated with the oil content of the reservoir. Where the lithology of the reservoir is good, the porosity and permeability values of the reservoir are high, and the oil content level of the reservoir is high. In addition, the density value and neutron value of the reservoir with high oil content level are low.

(2) Research on logging interpretation models for reservoir parameters shows that there is a good relationship between density and porosity based on the porosity logging interpretation model, with a correlation coefficient of 0.86; The permeability logging interpretation model found that the permeability is mainly distributed around the regression line of 45°; By determining the formation resistivity and using Archie's formula to determine the limit of water saturation in the reservoir, the water saturation of the reservoir is less than 50%; The water saturation of the same oil water layer is greater than 50% and less than 70%; The water saturation of the oil bearing water layer is greater than 70% and less than 80%; The water saturation of the water layer is greater than 80%.

(3) Through comprehensive analysis of mercury intrusion method, oil bearing occurrence method, oil testing analysis method, and cumulative frequency statistics, the lower limit standard of effective reservoir physical properties in the study area is: porosity is 7%, permeability is 0.05mD; By using the fluid identification chart, the lower limit standard for effective reservoir electrical properties is determined as follows: acoustic transit time is 63 $\mu\text{s}/\text{ft}$, with a density of 2.25 g/cm^3 .

Acknowledgements

This work was financially supported by the National Natural Science Foundation of China (42002154) and Open Fund Project of Heilongjiang Key Laboratory of Oil and Gas Reservoir Formation Mechanism and Resource Evaluation (KL20190101). The authors would like to thank the editor and the reviewers of this paper for their valuable comments that helped improve the quality of the paper.

References

1. Li Zandong, Bao Chuhui, Wang Dianju, et al. Controlling effect of structure palaeogeomorphology for sand bodies of Wuerxun—Beir Sag in Haila-er Basin[J]. *Journal of Central South University Science and Technology*, 2016, 47(7):2357-2365.
2. Wu Haibo, Li Junhui, Liu He. Formation condition and distribution rule of lithologic and stratigraphic reservoirs in Wuerxun—Beir Sag[J]. *Journal of Central South University Science and Technology*, 2015, 46(6):2178-2187.
3. Zhang Chen, Wei Kuisheng. Characteristics and reservoir formation condition in the southern Wuerxun Depression[J]. *Acta Petrolei Sinica*, 2005, 26(2):47-52.
4. Zhang Chen, Li Chunbai, Chu Meijuan, et al. Analysis on Characteristics and Controls of High-Frequency Sequences of Lower Cretaceous Series in Wuerxun Depression[J]. *Acta Sedimentologica Sinica*, 2005, 23(4):657-663.
5. Fang Wei. Reservoir characteristics of the first member of the south Wudong slope belt in Wuerxun depression[J]. *Journal of Yangtze University Science and Technology*, 2013, 10(7):16-17.
6. Liu Yiming, Ye Jiaren, Zhang Fei, et al. Fluid Identification and Evaluation of Tight Sandstone Reservoir in Es2 of Qibei Slope Belt in Qikou Sag[J]. *Earth Science*, 2022, 47(5):1762-1776.
7. Yin Hongrong, Zhou Hu, He Weiqing, et al. Logging parameter interpretation model and the lower limit standard for reservoir evaluation of Chang 82 reservoir in Zhuang 9 Well Block of Heshui Oilfield[J]. *Journal of Yangtze University Science and Technology*, 2021, 18(2):36-41.
8. Li Yingxu, Zhao Junxing, Wei QianSheng, et al. The reservoir“four properties”relation and the lower limit of effective reservoir in He 1 Member of Xiashihezi Formation in central area of Hangjinqi, Ordos Basin, China[J]. *Journal of Chengdu University of Technology: Science & Technology Edition*, 2021, 48(6):675-682+731.
9. Chen Luoyuan, Qian Yugui, Liao Luyao, et al. COMPREHENSIVE EVALUATION OF HE7 EFFECTIVE RESERVOIR OF MIDDLE PERMIAN LOWER SHIHEZI FORMATION IN WELL BLOCK OF SU-14 OF SULIGE GAS FIELD[J]. *Mineralogy and Petrology*, 2021, 41(2):109-117.
10. Hui Zengbo, Sun Mengsi, Feng Congjun, et al. Study on four reservoir characteristics and oil-water layer identification of the third member of the east Cha71 fault block in Chaheji oilfield[J]. *World Well Logging Technology*, 2021, 42(2):56-59.
11. Liu Chengchuan, Chen Jun, Li Huaji, et al. Logging evaluation of the tight sandstone reservoir in the gas reservoir of the Shaximiao formation within Zhongjiang gas field, China[J]. *Geophysical Prospecting For Petroleum*, 2020, 59(1):131-140.
12. Chen Jia, Feng Congjun, Yu Tianjun, et al. The lower limit of physical properties of tight reservoir in He 8 Member of Y113-Y133 gas well area, Yanchang Gas Field, Ordos Basin[J]. *Natural Gas Geoscience*, 2022, 33(6):955-966.
13. Zhang Shiming, Wang Jiangong, Zhang Yongshu, et al. Determination of petrophysical property cutoffs of lacustrine dolomite intercrystalline pore reservoir in the Xiaganchaigou Formation, western Qaidam Basin [J]. *Acta Petrolei Sinica*, 2021, 42(1):45-55+118.
14. Zhou Nengwu, Lu Shuangfan, Wang Min, et al. Limits and grading evaluation criteria of tight oil reservoirs in typical continental basins of China[J]. *Petroleum Exploration and Development*, 2021, 48(5):939-949.
15. [15] Meng Lei. Lower Limits of Physical Properties of Sandstone Reservoirs in the Second Member of Sangonghe Formation in Moxizhuang Oilfield[J]. *Xinjiang Petroleum Geology*, 2020, 41(5):557-564.
16. Lu Feng, Wang Jian, Zhang Juan, et al. Characteristics and lower limit of physical properties for reservoirs of 1st Member of Sangonghe Formation in Mosuowan area[J]. *Fault-Block Oil & Gas Field*, 2021, 28(3):300-304.
17. Zhang Yiming, Fu Xiaodong, Guo Yongjun, et al. Petrophysical property limits of effective tight oil reservoirs in the lower part of the first member of Cretaceous Tengger Formation, A'n'an Sag, Erlian Basin, North China[J]. *Petroleum Geology & Experiment*, 2016, 0(4):551-558.
18. Cai Zhendong, Zhao Chenyang, Du Yu, et al. Study on the Effective Thickness of Yan 10 Reservoir in M Area of Ordos Basin Maling Oil Field [J]. *Liaoning Chemical Industry*, 2015, 0(4):451-455.
19. Bai Ze, Tan Maojin, Shi Yujiang, et al. Genesis of low-resistivity oil pays and a fluid identification method for tight sandstone reservoirs: A case study of the Chang 8 Formation in the Longdong West area, Ordos Basin[J]. *Geophysical Prospecting For Petroleum*, 2022, 61(4):750-760.
20. Zhang Congxiu, Hao Jinmei, Liu Zhiheng, et al. A Study on the Logging-Based Identification Method for Reservoir Fluid Properties of the Yan'an Formation in the Huanxi—Pengyang[J]. *Petroleum Drilling Techniques*, 2020, 48(5):111-119.